

# Automatic ROI Specification and Reference Frame Selection for Motion Correction in Cardiac Imaging

Jieying Luo<sup>1</sup>, R. Reeve Ingle<sup>1</sup>, and Dwight G. Nishimura<sup>1</sup>

<sup>1</sup>Electrical Engineering, Stanford University, Stanford, California, United States

**Target Audience:** MR engineers, physicists and clinicians interested in cardiac imaging, object detection and motion correction.

**Purpose:** Recent coronary artery studies have realized free-breathing multiphase whole-heart coronary MR angiography with a 3D cones non-Cartesian trajectory<sup>[1]</sup>. Respiratory motion of the heart is tracked and retrospectively corrected using sagittal and coronal 2D image navigators acquired with a fast 2D interleaved spiral sequence at every heartbeat. These 2D image navigators can track motion along all three major axes and lead to better motion correction. An ROI covering the heart and a reference image are required to be manually specified for the motion estimation. In this work, an automatic method for determining the ROI specification and reference frame selection was developed, enabling fully-automated motion correction of cardiac images.

**Methods:** There are many existing methods for heart detection. Common approaches use the Hough transform in short-axis images<sup>[2-3]</sup> and cannot be directly applied to the navigator images in coronal and sagittal planes. After selecting a reference sagittal and coronal navigator image (described below), we use a combination of filtering and feature region searching techniques to detect a rectangular ROI covering the heart. This ROI is used by a least-squares technique to estimate SI, AP, and RL motion<sup>[1]</sup>. In the coronal plane (Fig. 1), the LR boundaries are obtained with a customized convolution filter (white box with  $\pm 1$ ). The inferior boundary is obtained by detecting the low-intensity feature region between the heart and the diaphragm (yellow box). The superior boundary is detected by searching the red line with at least 40% (empirical value) of pixels in that row exceeding the mean intensity. In the sagittal plane (Fig. 2), the SI boundaries are the same as those found for the coronal plane, assuming that the offset of the imaging center is negligible between coronal and sagittal images. The posterior boundary is detected with a convolution filter, and the anterior boundary is obtained by detecting the low-intensity feature region between the heart and the chest.

The least-squares motion estimation technique requires that one of the navigator images be used as a reference. Navigator images acquired at end expiration are desirable reference images because there is very little respiratory motion during this period. We use an efficient principal component analysis technique to locate an end-expiration reference frame (Fig. 3). First, the sagittal and coronal navigator images are reformatted into  $n \times m$  matrices, where  $n$  is the number of pixels per image and  $m$  is the number of navigator images. Next, singular value decomposition is performed. The leading right singular vector tracks temporal intensity changes of the navigator images, and it correlates very closely with respiratory motion. Histogram analysis is performed on the right singular vectors to locate a reference time frame with both sagittal and coronal navigators at end expiration.

**Results and Discussion:** The automatic method has been applied to eleven patient and volunteer datasets. The navigator images have FOV = 28 cm and resolution = 3.2 mm. There is large variation between these datasets in terms of shape and size of the heart, image intensity, chest thickness, etc. In some datasets, the motion estimate is sensitive to ROI specification and sometimes yields large outliers. A histogram analysis technique was developed to automatically detect these outliers, and the motion estimation is repeated using a slightly enlarged or contracted rectangular ROI or a different reference frame at end expiration. The automatic method is successful in all eleven datasets, even correctly identifying the heart in images with large spiral aliasing artifacts (Fig. 4). Motion estimates obtained from these ROIs agree well with manual selection (e.g., Fig. 5). Only minor shifting and scaling exist between motion estimates derived from automatic and manual selection. Finally, when using the motion estimates to correct the acquired image data, the resulting image quality is comparable to that obtained with a manually optimized ROI and reference frame (Fig. 6).

**Conclusion:** An automatic method for specifying an ROI covering the heart and reference frame selection has been developed, which enables the automation of motion correction in the free-breathing multiphase coronary MR angiography. This method is verified using eleven volunteer and patient datasets, achieving image quality that is comparable with a manually optimized ROI and reference frame.



**Figure 1.** ROI in coronal plane. LR boundaries are obtained using a customized convolution filter (white box with  $\pm 1$ ). Inferior boundary is obtained by detecting the low-intensity feature region between heart and diaphragm (yellow box). Superior boundary is detected by searching the red line with at least 40% pixels exceeding mean intensity.

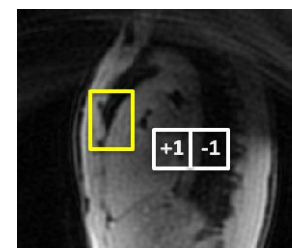


**Figure 2.** ROI in sagittal plane. Posterior boundary is obtained using a convolution filter (white box with  $\pm 1$ ). Anterior boundary is obtained by detecting feature region between heart and chest (yellow box).

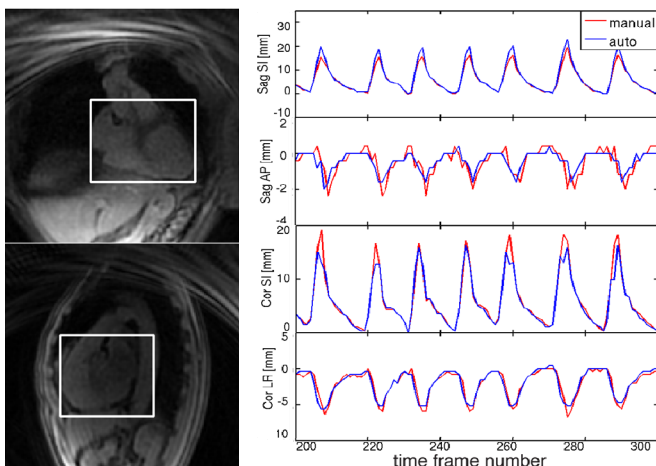


**Figure 4.** Successful ROI specification for the heart. **Figure 5.** Motion trajectories obtained automatically and manually, in good agreement.

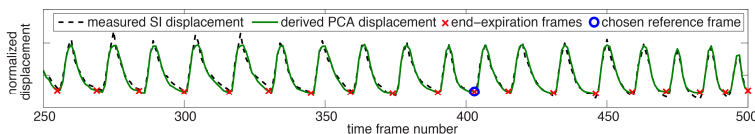


**Figure 3.** Automatic reference frame selection using principal component analysis.

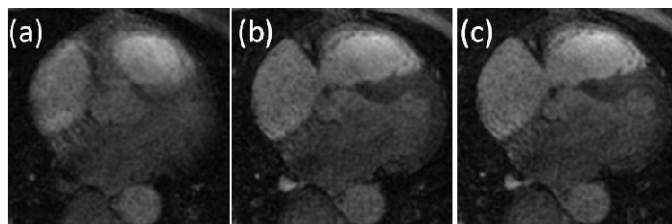


**Figure 6.** Reconstructed images (a) without motion correction, and with motion correction (b) automatically or (c) manually. The automatic result is comparable to manual selection, with a large reduction of motion blurring compared to (a).

**References:** 1. Wu HH, et al. MRM early view, 2012. 2. Brejl M, et al. IEEE TMI 19(10): 973-985, 2000. 3. Cocosco C, et al. Proc. CARS, p. 1126, 2004. 4. Pavani SK, et al. Patt. Recog. 43 (1): 160-172, 2010.